

## Research Article

# An Opportunistic Error Correction Layer for OFDM Systems

Xiaoying Shao, Roel Schiphorst, and Cornelis H. Slump

The Signals and Systems Group, Department of Electrical Engineering Mathematics and Computer Science (EEMCS),  
University of Twente, 7500 AE Enschede, The Netherlands

Correspondence should be addressed to Xiaoying Shao, x.shao@ewi.utwente.nl

Received 29 July 2008; Revised 7 November 2008; Accepted 14 January 2009

Recommended by Alister G. Burr

We propose a novel cross layer scheme to reduce the power consumption of ADCs in OFDM systems. The ADCs in a receiver can consume up to 50% of the total baseband energy. Our scheme is based on resolution-adaptive ADCs and Fountain codes. In a wireless frequency-selective channel some subcarriers have good channel conditions and others are attenuated. The key part of the proposed system is that the dynamic range of ADCs can be reduced by discarding subcarriers that are attenuated by the channel. Correspondingly, the power consumption in ADCs can be decreased. In our approach, each subcarrier carries a Fountain-encoded packet. To protect Fountain-encoded packets against bit errors, an LDPC code has been used. The receiver only decodes subcarriers (i.e., Fountain-encoded packets) with the highest SNR. Others are discarded. For that reason a LDPC code with a relatively high code rate can be used. The new error correction layer does not require perfect channel knowledge, so it can be used in a realistic system where the channel is estimated. With our approach, more than 70% of the energy consumption in the ADCs can be saved compared with the conventional IEEE 802.11a WLAN system under the same channel conditions and throughput. In addition, it requires 7.5 dB less SNR than the 802.11a system. To reduce the overhead of Fountain codes, we apply message passing and Gaussian elimination in the decoder. In this way, the overhead is 3% for a small block size (i.e., 500 packets). Using both methods results in an efficient system with low delay.

Copyright © 2009 Xiaoying Shao et al. This is an open access article distributed under the Creative Commons Attribution License, which permits unrestricted use, distribution, and reproduction in any medium, provided the original work is properly cited.

## 1. Introduction

The wireless channel is a very hostile environment. Therefore, it is a challenge to communicate both reliably and with a high throughput. In this paper, we investigate a novel error-correction layer based on *Fountain codes*, *orthogonal frequency-division multiplexing* (OFDM), and adaptive analog-to-digital conversion to mitigate the effects of a wireless channel at a lower power consumption compared to traditional solutions.

OFDM has become a popular scheme for recent WLAN standards which operate at a high bit rate [1–3]. The main advantage of OFDM over the single-carrier scheme is its ability to eliminate *inter-symbol interference* (ISI) without complex equalization filters in the receiver [4]. OFDM has a high *peak-to-average power Ratio* (PAPR), therefore it requires *analog-to-digital converters* (ADC) with a high dynamic range. These high-resolution ADCs can take up to 50% of the baseband power [5].

In the current generation of WLAN equipment (based on IEEE 802.11a [6]), the *forward error-correction* (FEC) layer is based on *rate compatible punctured codes* (RCPC). These codes have good performance for random bit-errors, but poorer performance for burst bit errors. For that reason, an interleaver is applied to randomize the burst errors of the wireless channel. On the other hand, the wireless channel is changing in time. This means that some packets are received with a “good” channel and others over a “bad” channel. The error-correction layer based on RCPC has been designed in such a way that for most channel realizations the *bit-error rate* (BER) is zero. For a small part of the channel, bit errors will occur and retransmission is necessary. Although this solution works well in practical systems, it is not energy-efficient for two reasons.

- (i) Packets which have encountered “bad” conditions are still processed by the entire receiver chain.
- (ii) Fixed high-resolution ADCs are used in the current WLAN systems, designed for worst-case scenarios.

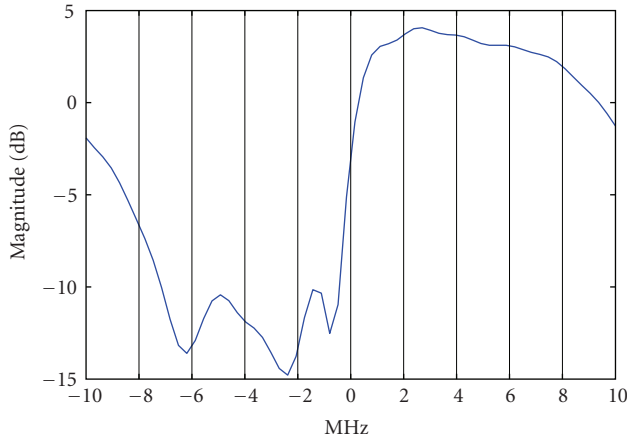


FIGURE 1: Example of the baseband transfer function of a frequency-selective channel *model A*.

In this paper we propose a new error-correction layer, which does not have these disadvantages. It is an opportunistic error correction layer because it processes only “good” packets. Also, it is a low power-consumption scheme as the resolution of the ADC is adapted to the minimum for each scenario instead of being designed for worst-case situations.

A further resolution reduction of the ADC can be achieved by discarding those parts of the channel with deep fading. Taking Figure 1 as an example, the dynamic range of the whole channel is around 18.8 dB. From this figure, we can see that deep fading does not happen everywhere and only occurs in the frequency band of  $-8 \sim 0$  MHz. By discarding this 8 MHz sub-band, the dynamic range of the channel is reduced to around 10.4 dB. The current WLAN standards do not support this approach, as all sub-bands are considered equally important by the FEC layer.

Therefore, we propose a novel FEC layer based on Fountain codes that allows us to discard those parts of the channel with deep fading. In [7], MacKay describes the encoder of a Fountain code as a metaphorical fountain that produces a stream of encoded packets. Anyone who wishes to receive the encoded file holds a bucket under the fountain and collects enough packets to recover the original data. It does not matter which packets are received, only a minimum amount of packets have to be received correctly [7]. In other words, the Fountain-encoded packets are independent with respect to each other.

To apply Fountain codes in WLAN systems, we divide a block of source bits into a set of packets which are encoded by a Fountain code. A Fountain-encoded packet is transmitted over a subcarrier. Thus, multiple packets are transmitted simultaneously, using frequency division multiplexing. In our system the transmitter generates an abundance of packets and the receiver can discard Fountain-encoded packets which are transmitted over the subcarriers with deep fading. Correspondingly, the power consumption in the ADCs decreases.

The proposed method is an opportunistic error correction layer because it does not process all received packets but

only processes “good” packets. This error-correction is able to cope with discarding packets because Fountain-encoded packets are independent of each other. Also, less power is consumed as the resolution of the ADC is adapted to the minimum required in each case, compared to using a fixed-resolution ADC. Thus, it is a novel cross-layer approach which integrates the error-correction into the physical layer of an OFDM system.

The outline of this paper is as follows. We propose two techniques which together form the new error-correction layer and reduce the power consumption: Fountain codes and a resolution-adaptive ADC. First, Fountain codes are discussed, which is followed by the resolution-adaptive ADC. A practical example is given in this paper considering the IEEE 802.11a system. In Section 4, a description is given of the IEEE 802.11a system model and are included our proposed modifications. Finally, the simulation results are described, which compare the conventional 802.11a system with our modifications. The paper ends with conclusions and future work.

## 2. Fountain Codes

The proposed error-correction layer is generic: any Fountain codes (e.g., *Luby Transform* (LT) codes [8], Raptor codes [9], etc.) can be applied in it. In this paper, we use LT codes in the proposed error-correction layer.

Consider a file of size  $K$  packets  $s_1, s_2, \dots, s_K$  to be encoded by a Fountain code. A “packet” has  $m$  bits and is considered as an elementary unit here. At each clock cycle, indexed by  $n$ , the encoder randomly chooses several packets, and computes the bitwise sum (XOR) of these source packets to generate the corresponding transmitted packet. The number of packets used is random, as well as the selection of the packets used. The Fountain code can supply us with a stream of packets based on source packets  $s_1, s_2, \dots, s_K$ . In practical situations, however, only a fixed number of packets  $N$  are generated.

At the receiver side enough packets have to be received for successful decoding. The required number of received packets  $N$  is slightly larger than the number of source packets  $K$  and is defined by

$$N = K(1 + \varepsilon), \quad (1)$$

where  $\varepsilon$  is the percentage of extra-packets and is called the overhead.

After receiving  $N$  packets, the receiver can recover the source packet using the *message-passing* algorithm which has a linear decoding cost. By using message-passing to decode LT codes, the practical block size for LT codes with small  $\varepsilon$  (e.g., within 5%) is on the order of  $10^4$  or higher, which prevents the Fountain scheme from efficiently supporting real-time applications (i.e., low delay) [10]. For low failure probability (e.g., 1%), using message-passing decoding, the practical overhead for small block size (i.e., on the order of  $10^3$ ) is much larger than in theory [7]. In [11], the authors show that the practical overhead of LT codes is 14% when  $K = 2000$ , which limits the application of

LT codes in practical systems to  $K \leq 2000$ . The practical overhead becomes smaller for a larger number of source packets. Although larger packets decrease the overhead, this also results in more delay. In addition, if the message-passing decoding fails, it does not mean that the source packets are not recoverable. Gaussian elimination can also be used for decoding, if the matrix  $G$  can be transformed into an up-converted matrix.

However, Gaussian elimination has higher complexity compared to the message-passing algorithm. The decoding cost of using the message-passing algorithm scales as  $K \log_e K$  and the cost of using the Gaussian elimination algorithm is on the order of  $K^3$  [7]. In [12], the authors propose a fast Gaussian elimination algorithm over GF(2) with reduced cost  $O(K^2)$ . The message-passing algorithm has lower decoding costs (computational complexity) but requires more overhead (i.e., Fountain-encoded packets) for successful decoding compared to the Gaussian elimination. Therefore, we can combine both methods to give low overhead and a reasonable complexity. Gaussian elimination is applied after the message-passing algorithm. Packets which cannot be retrieved by message-passing will be decoded by Gaussian elimination. By using both methods, the number of source packets can be small and the practical overhead is reduced as shown in Figure 2. From this figure, we can see that the overhead of using the message-passing plus Gaussian elimination for  $K = 500$  can be reduced from 42% to 3% in comparison to only message-passing decoding. Furthermore, the complexity of this scheme is increased to  $O(K_1 \log_e K_1) + O(K - K_1)^2$ , where  $K_1$  is the number of source packets recovered by the message-passing algorithm and  $K - K_1$  is the number of source packets recovered by the Gaussian elimination algorithm. For  $K = 500$ , on average around 250 source packets can be decoded by the message-passing algorithm and the rest of the packets can be recovered by Gaussian elimination. In this case, the complexity is around  $6 \times 10^4$ , which is around 25% of the complexity of only using Gaussian elimination algorithm for decoding. However, the overhead by using both methods can be reduced from 42% to 3% compared with the overhead of only using message-passing.

As mentioned before, Fountain-encoded packets are assumed to be transmitted over the *erasure channel*, which means that the encoded packet is either received error-free or not received at all. However, wireless channels are not erasure channels. To convert the wireless channel into an erasure channel, *error-correction codes* are applied to each Fountain-encoded packet in practical systems [7]. Both the *Low Density Parity Check* (LDPC) codes [13] and Turbo codes [14] are good error-correction codes which allow the transmission data rate close to the Shannon limit, but the complexity of LDPC codes is lower than Turbo codes and the performance of LDPC codes is better than Turbo codes for short-length blocks [15]. Therefore, in this paper LDPC codes are used together with *Cyclic Redundancy Check* (CRC) to make the wireless channel behave like an erasure channel.

Our FEC encoding scheme is performed as follows. First, a Fountain-encoded packet is created. Then, a CRC is added.

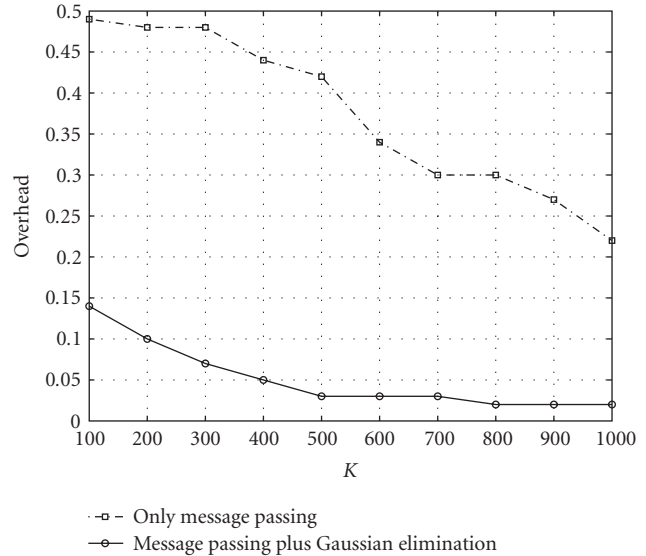


FIGURE 2: The overhead of Fountain codes (LT codes,  $c = 0.03$ ,  $\delta = 0.3$ ). Fountain-encoded packets are transmitted over the erasure channel with the erasure probability of 20%. The dash-dot curve is the overhead of LT codes only using message-passing decoding and the solid curve is the overhead of LT codes using message-passing algorithm and Gaussian elimination together to decode.

Finally, the packet is encoded by an LDPC code to combat bit errors introduced by the channel.

At the receiver, each Fountain-encoded packet is first LDPC decoded if its energy is equal to or higher than a threshold (i.e., corresponding to  $\text{BER} \leq 10^{-5}$ ). The received packet is discarded if its energy is below the threshold. If the LDPC decoding fails, the received packet is discarded as well. If the LDPC decoding succeeds, the CRC is used to identify any errors undetected by the LDPC codes. If the CRC decoder detects an error, the receiver assumes that the whole packet has been lost. Once the receiver gets  $N$  surviving Fountain-encoded packets, it starts to recover the source data.

### 3. Resolution-Adaptive ADC

Wireless channels in OFDM systems are fading channels and are modeled as frequency-selective channels [4, 16]. An example is depicted in Figure 1. If a “bad” channel (A “bad” channel means in our definition a large difference in energy between subcarriers, that is, a large dynamic range of the ADC is required.) is encountered, the required dynamic range of the ADC is higher than for a “good” one. (A “good” channel on the other hand is when, e.g., flat fading occurs.) In addition, the ADC power consumption can be almost 50% of the total baseband power consumption [5]. This means that a resolution-adaptive ADC can potentially save power. A CMOS implementation of such an ADC is described in [17]. In this implementation, the power consumption scales linearly with the number of quantization levels.

**3.1. Minimum Number of Quantization Levels.** In OFDM receivers, demodulation of the subcarriers is performed in the frequency domain. For that reason, it is not beforehand clear, how many ADC bits are necessary for proper decoding. In [18], the authors have derived a relation between the quantization noise in the time domain and frequency domain. However, results are shown only for nonfading channels. In this section, we present a scheme to design an optimum low-resolution ADC for frequency-selective channels.

Because the quantization noise depends on the signal, we first analyze the statistical characteristics of the ADC input  $r_n$ . The channel is supposed to be noiseless, so the output at the  $n$ th moment  $r_n$  is defined as

$$r_n = \sum_{l=0}^{L-1} h_l x_{n-l}, \quad (2)$$

where  $L$  is the number of channel taps,  $h_l$  the channel taps, and  $x$  the transmitted signal. We assume that the quantization noise is dominant, so other noise (e.g., thermal noise) is ignored in this paper. From [18], we know that  $x_n$  can be modeled as a complex Gaussian-distributed random variable with zero-mean and a variance of 1. The elements in vector  $[x_0, x_1, \dots, x_{N-1}]$  are mutual independent.

According to the *central limit theorem* [19], the sum of a sequence of independent, identically distributed random variables tends to be Gaussian-distributed, so the probability density function of  $r_n$  can be described as

$$f(r_n) \approx \frac{1}{\pi} e^{-|r_n|^2 / \sum_l |h_l|^2}. \quad (3)$$

In other words,  $r_n \sim \mathcal{CN}(0, \sum_l |h_l|^2)$ .

The ADC output  $y_n$  is expressed by

$$y_n = \mathcal{Q}(r_n) = \sum_l h_l x_{n-l} + n_n, \quad (4)$$

where  $n_n$  is the quantization noise in the time domain. From [18], we know that  $n_n$  is uniformly distributed with zero mean and a variance of  $\Delta^2/6$ , where  $\Delta$  is the uniform quantization step.

Due to the additional cyclic prefix in each OFDM symbol, the convolution in (4) can be considered as a *cyclic convolution* [4]. So, after the OFDM demodulation, we can write  $Y_k$  as

$$\begin{aligned} Y_k &= \frac{1}{\sqrt{N}} \sum_n y_n e^{-j(2\pi/N)nk} \\ &= \frac{1}{\sqrt{N}} \sum_n \sum_l (h_l x_{n-l} + n_n) e^{-j(2\pi/N)nk} \\ &= \frac{1}{\sqrt{N}} \sum_n x_{n-l} e^{-j(2\pi/N)(n-l)k} \sum_l h_l e^{-j(2\pi/N)lk} \\ &\quad + \frac{1}{\sqrt{N}} \sum_n n_n e^{-j(2\pi/N)nk} \\ &= H_k X_k + N_k, \end{aligned} \quad (5)$$

where  $N_k$  is the quantization noise in the frequency domain and  $H_k$  is the fading over the  $k$ th subcarrier defined by

$$H_k = \sum_l h_l e^{-j(2\pi/N)lk}. \quad (6)$$

In [18], the authors have shown that  $N_k$  is a Gaussian-distributed random variable with zero mean and a variance of  $\Delta^2/6$ . Thus, for each subcarrier, the variance of the quantization noise is the same, but the signal-to-(quantization)-noise ratio (SNR) is different due to different fading:

$$\text{SNR}_k = \frac{|H_k|^2}{\Delta^2/6}. \quad (7)$$

Error correcting codes can be applied to mitigate the effects of quantization and each code has a certain SNR threshold to achieve BER at a certain order (e.g.,  $10^{-4}$ ) or lower. So, the quantization step  $\Delta$  can be determined once the error correcting code is chosen and the channel is estimated.

In practical systems, the ADC resolution is finite. This means that for the same channel, the required dynamic range of the ADC is larger for higher code rates.

If some clipping is allowed, the number of quantization levels  $N_q$  is given by [18]

$$N_q = 2 \left\lceil \frac{C}{\Delta} \right\rceil, \quad (8)$$

where  $C$  is equal to  $3\sigma_{r_n}$ . Once the channel is fixed,  $N_q$  is only dependent on  $\Delta$ . In such a case,  $\Delta$  depends not only on the applied error-correction codes in the system, but also on how the encoded bits are transmitted. Assume that the Fountain-encoded packets are transmitted over a wireless channel as shown in Figure 1 and that a packet is received correctly when  $\text{SNR} \geq 12$  dB. There are two schemes to transmit these Fountain-encoded packets

- (i) Scheme I is to transmit each packet over all subcarriers like current WLAN systems, which means that the SNR of the worst subcarrier should be at least equal to 12 dB. In this case, the required number of quantization levels  $N_q$  is 54 for the example in Figure 3.
- (ii) Scheme II is to transmit each packet over one subcarrier. Since each Fountain-encoded packet is independent, it does not matter if we discard some packets which are transmitted over “bad” subcarriers. From Figure 3, we can see that by discarding 15 subcarriers,  $N_q$  can be reduced to 38 in comparison to Scheme I.

**3.2. Power Consumption.** The power consumption of the ADC is proportional to the number of quantization levels  $N_q$  which is related to the effective number of bits (ENOB) by

$$N_q = 2^{\text{ENOB}}. \quad (9)$$

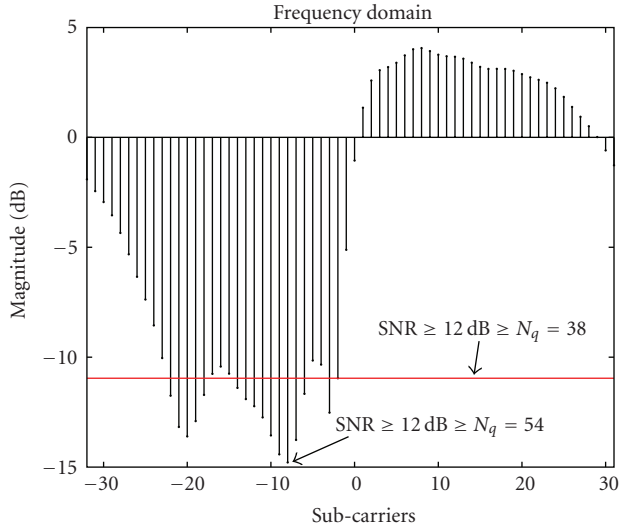


FIGURE 3: The difference in the number of ADC levels  $N_q$  between the transmission Scheme I and the transmission Scheme II. In this example,  $N_q = 54$  levels are required for the transmission Scheme I such that each Fountain packet is transmitted over all subcarriers;  $N_q$  can be reduced to 38 levels when 15 subcarriers are discarded in the transmission Scheme II where each Fountain packet is transmitted over one subcarrier only.

Thus,  $N_q$  is a measurement for the power consumption:

$$P = \sum_{i=0}^{M_c-1} \alpha_i N_{qi} \mathcal{M}, \quad (10)$$

where  $M_c$  is the number of channel realizations,  $\alpha_i$  is the percentage of the  $i$ th channel realization where useful information is transmitted,  $N_{qi}$  is the number of quantization levels used in the  $i$ th channel realization, and  $\mathcal{M}$  is the number of samples per MAC frame.

When Scheme II is applied, the power consumption of the ADC can be reduced by discarding “bad” subcarriers. However, discarding transmitted packets over “bad” subcarriers leads to an increase in the number of the transmitted packets. Therefore, there is a tradeoff in the power consumption of the ADC between the number of lost subcarriers and the number of transmitted packets.

So far, we have designed the quantization scheme for OFDM systems over the frequency-selective channels under the assumption of the perfect channel knowledge. However, in practical systems, the channel cannot be perfectly estimated, which affects the design of quantization scheme. We will discuss this influence in the following section.

#### 4. System Model

As mentioned earlier, our opportunistic error-correction layer is based on Fountain codes and resolution-adaptive ADCs which have been explained in the previous sections. This proposed error-correction layer can be applied in OFDM systems. The IEEE 802.11a system is taken as an example of an OFDM system in this paper.

In this section, the system model of an IEEE 802.11a transceiver is discussed as shown in Figure 4. It is a simplified model with focus on the (de)modulation and (en/dec)oding of the bit stream. This means that we assume, for example, that there is no adjacent channel interference.

The FEC layer in current IEEE 802.11a system is based on RCPC. RCPC has a good performance for random bit errors. An Interleaver is used to remove the burst errors. Although this solution works well in practical systems, it is not optimal. First, packets that have encountered a “bad” channel condition are still processed by the entire receiver chain. Although the IEEE 802.11a standard uses a form of adaptive modulation, it only consists of 6 modes which is a very coarse form. The transmitter tries continuously to use the highest code rate, but adaptation is relatively slow and each mode is designed for the “average” channel. This means that for most packets, the code rate and hence capacity can be increased. Furthermore, the resolution of the applied ADCs is fixed for a 802.11a system.

In Figure 5, we show the new error-correction layer that mitigates both problems. The key idea is to generate additional packets by the Fountain encoder. First, the source packets are encoded by the Fountain encoder. Then, a CRC checksum is added to each Fountain-encoded packet and LDPC encoding is applied. The code rate of the LDPC code is chosen relatively high as only packets with high SNR have to be decoded, others are discarded. Each encoded packet is transmitted on one subcarrier of the OFDM system. At the receiver side, we assume that the synchronization is perfect and the channel is estimated by an adaptive ADC with high-resolution. After that, the adaptive ADC can be reduced to the minimum necessary resolution for each channel realization. In the transmitter, more Fountain-encoded packets are created than necessary for decoding. The receiver has now the freedom to discard some of the received packets. A further resolution reduction can be achieved by discarding the packets which are transmitted over “bad” subcarriers.

If the SNR of the subcarrier is equal to or above the threshold, the received Fountain-encoded packet will go through LDPC decoding, otherwise it will be discarded. In our implementation, we choose a threshold of 12 dB for the used LDPC code. This means that the receiver is allowed to discard several subcarriers (i.e., packets) to lower the dynamic range of the ADC and hence the power consumption. After the LDPC decoding, the CRC checksum is used to discard erroneous packets. As only packets with a high SNR are processed by the receiver, this will not happen very often.

In practical systems, the channel cannot be perfectly estimated. High-resolution ADCs are applied to estimate the channel and the channel is estimated, for example by the *zero forcing* algorithm. A set of training symbols defined in [6] is used to estimate the channel, so we have:

$$Y_t = H_k X_t + N_h, \quad (11)$$

where  $X_t$  is the training symbol,  $Y_t$  is the received training symbol,  $H_k$  is the  $k$ th subcarrier, and  $N_h$  is the quantization

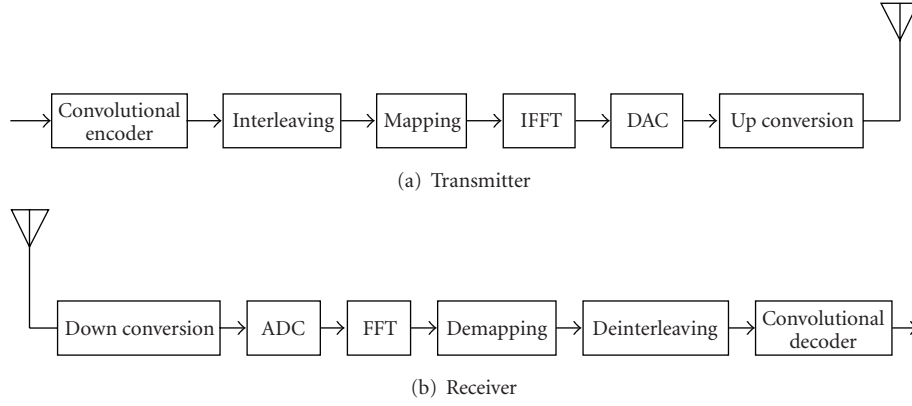


FIGURE 4: Conventional 802.11a (a) transmitter and (b) receiver.

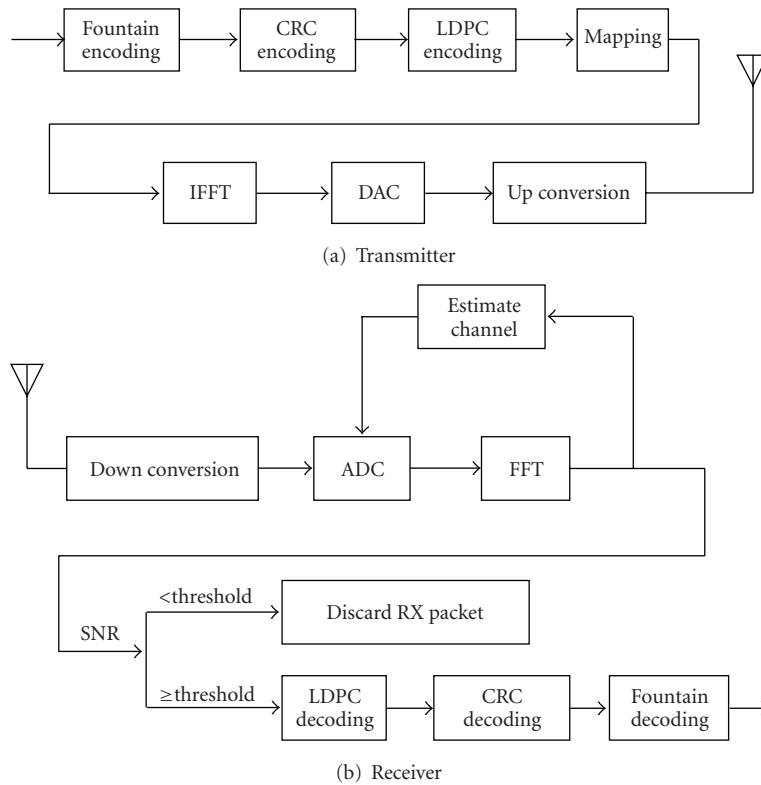


FIGURE 5: Proposed 802.11a (a) transmitter and (b) receiver. In the transmitter, first source packets are encoded by Fountain codes then LDPC and CRC are applied to each Fountain-encoded packet; after that each encoded packet is transmitted over a subcarrier. In the receiver, the channel is first estimated by high-resolution ADCs then the resolution of ADCs are adapted to the minimum according to the estimated channel knowledge. Each received packet is decoded by LDPC and CRC if  $\text{SNR} \geq \text{threshold}$ , otherwise, it will be discarded. When the receiver gets  $N$  Fountain-encoded packets, it can recover the source file.

noise from adaptive ADCs with high-resolution. The  $k$ th subcarrier can be estimated by

$$\begin{aligned} \hat{H}_k &= \frac{Y_t}{X_t} \\ &= H_k + \frac{N_h}{X_t}. \end{aligned} \quad (12)$$

So, we can rewrite the output signal in the frequency domain after quantization defined in (5) as

$$\begin{aligned} Y_k &= H_k X_k + N_a \\ &= \hat{H}_k X_k - \frac{N_h}{X_t} X + N_a \\ &= \hat{H}_k X_k + N', \end{aligned} \quad (13)$$

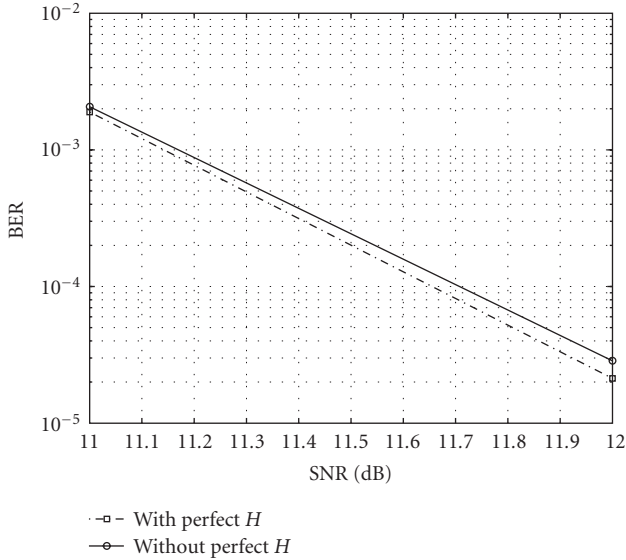


FIGURE 6: BER of the (175,255) LDPC code. The dash-dot line is the BER curve with perfect channel knowledge and the solid line is the BER curve without perfect channel knowledge.

where  $N_a$  is the quantization noise from resolution-adaptive ADCs. The variance of  $N'$  ( $\sigma_{N'}^2$ ) is equal to  $\sigma_{N_h}^2 + \sigma_{N_a}^2$ . Therefore, with the channel estimation error, the SNR for each subcarrier defined in (7) can be updated as

$$\begin{aligned} \text{SNR}_k &= \frac{|\hat{H}_k|^2}{\sigma_{N'}^2} \\ &= \frac{|\hat{H}_k|^2}{\sigma_{N_h}^2 + \sigma_{N_a}^2} \\ &= \frac{|\hat{H}_k|^2}{\sigma_{N_h}^2 + \Delta^2/6}. \end{aligned} \quad (14)$$

As we can see, the noise defined in this equation is composed of the quantization noise from high-resolution ADCs for the channel estimation and from resolution-adaptive ADCs for the user data.

The channel estimation error will affect the SNR threshold for the correct LDPC decoding, as shown in Figure 6. From this figure, we can see that the BER degradation can be neglected (within 0.1 dB gap for BER at the order of  $10^{-5}$ ), which means the received packets can still go through the LDPC decoder when  $\text{SNR} \geq 12$  dB. Though the channel estimation error does not influence the LDPC decoding too much, the number of quantization levels  $N_q$  will be affected, as the LDPC decoder needs to know the SNR defined in (14). How  $N_q$  is influenced by the channel estimation error depends on the design method of quantization scheme. There are two design methods as follows.

- (i) Method I: Assume  $\sigma_a^2 > \sigma_h^2$  and the number of lost subcarriers is fixed, so the quantization step  $\Delta$  can be derived from (14) and defined as

$$\Delta = \sqrt{6 \frac{|\hat{H}_k|^2}{\text{SNR}_k} - \sigma_h^2} \quad (15)$$

and  $N_q$  can be determined by (8).

- (ii) Method II: Assume  $\sigma_a^2 \gg \sigma_h^2$ , (14) can be rewritten as

$$\text{SNR}_k = \frac{|\hat{H}_k|^2}{\Delta^2/6}, \quad (16)$$

so  $\Delta$  is defined as:

$$\Delta = \sqrt{6 \frac{|\hat{H}_k|^2}{\text{SNR}_k}}, \quad (17)$$

and  $N_q$  follows from (8) as well. In this case, we will have smaller  $N_q$  compared to Method I but we might lose more subcarriers (i.e., packets) since the SNR defined in (14) is smaller than the SNR we assume in (17).

In order to see the influence of the channel estimation error and the performance of the quantization design Methods I and II, we give an example as shown in Figure 7. In this example, we only consider 52 active subcarriers defined in [6] and assume that no subcarrier is discarded. In the case of perfect channel estimation, 248 quantization levels are required. When the channel is estimated by the zero forcing algorithm, the required  $N_q$  using Method I is 396, and using Method II, 216 levels are needed which is less than the case of perfect channel estimation. However, one extra subcarrier is discarded when Method II is applied, because this subcarrier has lower SNR than the threshold (i.e., 12 dB). Obviously, Method II requires smaller  $N_q$  in comparison with Method I though in this case we might lose more subcarriers than we expect. Method II is chosen to design the quantization scheme in this paper.

As we mentioned before, there is a tradeoff in the power consumption of ADCs between the number of lost subcarriers and the number of transmitted packets. In Figure 8 the relation is depicted between power consumption (dynamic range) and the number of discarded subcarriers with perfect channel knowledge and without. In each case the same amount of information was transmitted and decoded successfully by the receiver. Besides, the subcarriers with the lowest energy are discarded. From this figure, we can also see that the channel estimation error does not really affect the total power consumption. For the perfect channel estimation, the minimum power consumption is reached when 14 subcarriers are discarded. Without perfect channel knowledge, the lowest power consumption can be obtained when 15 subcarriers are discarded.

In the following section, we compare both systems for the same bit rate.

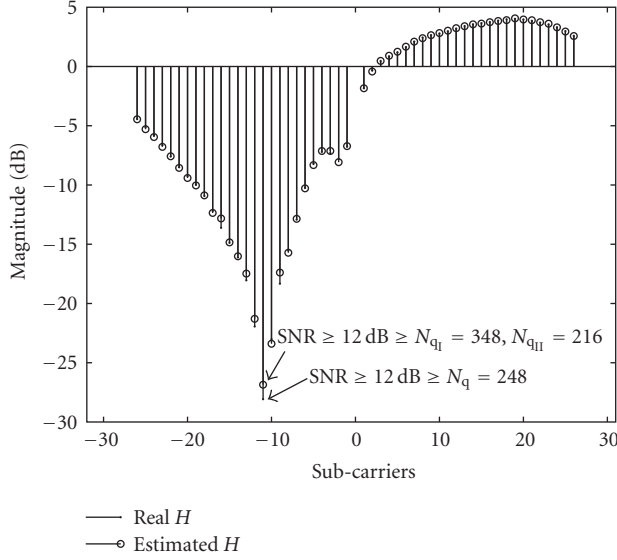


FIGURE 7: The influence of the channel estimation error and the difference in  $N_q$  between the quantization design Method I and the quantization design Method II. In this example, we assume the worst subcarrier has an SNR of 12 dB.  $N_q = 248$  for the case with perfect channel knowledge. With the estimated channel knowledge,  $N_q = 348$  for the quantization Method I and  $N_q = 216$  for the quantization Method II.

## 5. Performance Analysis

In this section we compare three scenarios. Channel *model A* is used in all our simulations and we simulate at least 1 million bits per simulation. The first scenario, Scenario I, is a conventional IEEE 802.11a system with 16-QAM modulation and code rate 1/2. This mode has a throughput of 24 Mbit/s (source bits). As the standard allows 10% packet loss [6], the effective throughput is  $0.9 \cdot 24 = 21.6$  Mbit/s. Moreover, we assume that conventional ADCs are used, of which the resolution has been designed for 90% of the channel realizations. In Scenario II, the conventional ADCs are replaced by resolution-adaptive ADCs, which are designed to allow 10% packet loss. Finally, in Scenario III, we apply the new opportunistic error-correction layer, which has the same effective throughput as Scenario II.

As discussed before, the channel estimation error can be neglected in case of using high-resolution ADCs. In our simulations, we use the parameters of Table 1. The “SNR in frequency domain” is the minimal SNR for each subcarrier. If this value is met, the packet error rate (PER) will be less than 10%, as required by the standard [6]. Symbols are transmitted in bursts (i.e., MAC frame) and in 802.11a, 500 OFDM symbols are packed into one burst.

From Figure 8, one can derive that the minimal power consumption for Scenario III will be reached if about 15 subcarriers can be discarded without perfect channel knowledge. So, the LDPC and CRC checksum have to be chosen in such a way that the total throughput is equal to Scenario I and about 15 subcarriers are discarded by the receiver.

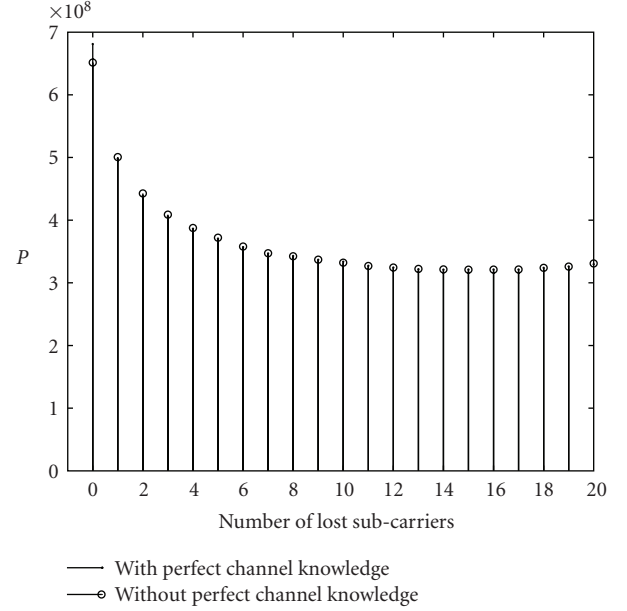


FIGURE 8: Power consumption defined in (10) versus the number of lost subcarriers for a Fountain code with a packet size of 168 bits. The dot points are with perfect channel knowledge and the circle points are without perfect channel knowledge.

TABLE 1: System setup comparison for three scenarios ( $N_c$ : the number of data carriers,  $N$ : the number of subcarriers,  $N_s$ : the number of symbols per MAC frame).

	Scenario I	Scenario II	Scenario III
ADC	normal	res. adapt.	res. adapt.
FEC	RCPC	RCPC	LDPC + Fount. codes
Code rate	0.5	0.5	0.66
Modulation	16-QAM	16-QAM	16-QAM
$N_c$	48	48	48
$N$	64	64	64
$N_s$	500	500	500
Effective throughput	21.6 Mbit/s	21.6 Mbit/s	21.6 Mbit/s
SNR in freq. domain	9.0 dB	9.0 dB	12.0 dB

We replace the error-correction layer by a 7-bit CRC checksum and an LDPC code (175,255) which has a code rate of 0.66. For the Fountain code part, we use a LT code with parameters  $c = 0.03$  and  $\delta = 0.3$ . The resulting Fountain code packets are transmitted on separate subcarriers and over multiple MAC frames. On average, 14 subcarriers can be discarded by the receiver, which is close to the optimal value if there is no perfect channel estimation.

Figure 9 shows the consumed power (per source bit) for each scenario versus the Fountain code block length  $K$  under the condition of the nonperfect channel knowledge. For each simulation point 2000 Fountain code bursts are transmitted. The power consumption in Scenario I is constant for each



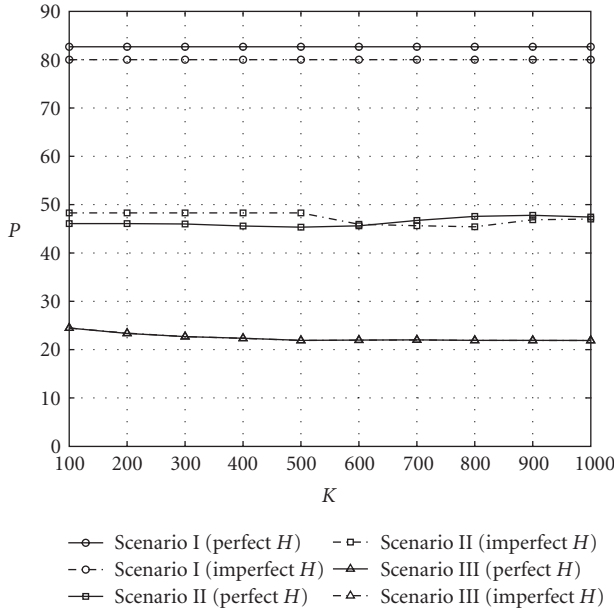


FIGURE 9: The power consumption (defined in (10)) per source bit. The curves with circle-mark are for Scenario I, the curves with square-mark are for Scenario II, and the curves with triangle-mark are for Scenario III. The solid curve is with perfect channel knowledge and the dash-dot line is without channel knowledge.

$K$  since the conventional ADC is designed for worst-case. In Scenario II, the power consumption on average is about 58% of the power consumed in Scenario I. The difference in the power consumption for different  $K$  in this scenario is due to the channel randomness. In Scenario III, the power consumption for different  $K$  is inversely proportional to the overhead of LT codes. The average power consumption for receiving 1 source bit in Scenario III is about 48% of the average power consumed in Scenario II and about 28% of the average power consumed in scenario I.

Furthermore, Figure 9 shows the power consumption with perfect channel knowledge. As we can see, for each Scenario, the consumed power has little difference between the perfect channel estimation and the nonperfect channel estimation. This difference depends on how accurate the channel is estimated. As we know, the zero forcing estimation algorithm assumes no noise in the received symbol which means this algorithm has better performance when SNR is higher. Figure 7 also shows that “good” subcarriers can be more accurately estimated than “bad” subcarriers. In Scenario III we only need to take care of “good” subcarriers but we have to take care of all subcarriers in Scenarios I, and II. From (8), we can see that  $N_q$  is determined by the quantization step  $\Delta$ . The threshold of the used LDPC is 12 dB which means  $\Delta$  depends on *the wanted subcarrier with the lowest energy*  $H_{k'}$  as defined in (14). In a word,  $N_q$  is determined by  $H_{k'}$ .  $|H_{k'}|^2$  in Scenario III is larger than  $|H_{k'}|^2$  in Scenario I and II. So, the difference in  $N_q$  between the perfect channel knowledge and the nonperfect channel knowledge is smaller in Scenario III than in Scenario I and II, as we can see in Figure 9. In this figure, in Scenario III both

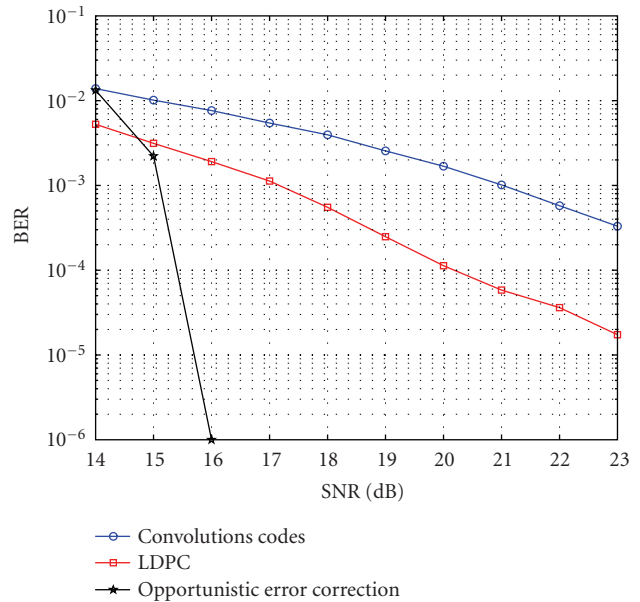


FIGURE 10: FEC layers comparison over channel *model A* with the same effective transmission data rate 21.6 Mbits/s (i.e., PER = 10%, BER =  $2 \times 10^{-4}$ ). The SNR is in the time domain and the channel estimation is assumed to be perfect. The blue circle points are for convolutions codes; the red square points are for LDPC codes from 802.11n and the black star points are for opportunistic error correction layer (Fountain codes + LDPC plus CRC). For SNR = 16 dB and higher, no errors are detected in the opportunistic error-correction layer. So, for SNR = 16 dB, we represent BER = 0 by  $10^{-6}$ .

curves overlap but this does not happen in Scenario I and II. Therefore, the new error-correction layer is less sensitive to the channel estimation error compared to the conventional error-correction layer.

Thus, the resolution-adaptive ADC can save around 42% power and the novel opportunistic error-correction layer can save an additional 30% power consumption. In total, the new method reduces the power consumption in ADCs by 72% compared to the current 802.11a standard.

From Section 3, we can see that low power consumption means low SNR requirement. Compared to the RCPC codes, LDPC codes have better performance close to the Shannon limit. For that reason, LDPC codes have been adopted by the IEEE 802.11n standard. In order to check how our scheme performs with respect to the required SNR, we compare convolutional codes, LDPC codes from the IEEE 802.11n standard and our opportunistic error correction layer under the condition of the same effective throughput (i.e., 21.6 Mbits/s). Figure 10 shows the simulation results over the noisy channel *model A* with perfect channel estimation when  $K = 500$ . For each simulation point, more than 1 million bits are transmitted. From this figure, we can see that the required SNR for convolutional codes is 23 dB when BER =  $2 \times 10^{-4}$ . A similar value for this channel model is reported in [20]. Figure 10 shows that LDPC codes have a gain of around 4 dB comparing to convolutional codes. However, the proposed method has a gain of around 7.5 dB.

## 6. Conclusions and Future Work

In this paper, we propose a novel cross-layer scheme which integrates the error-correction into the physical layer. This new opportunistic error-correction layer is designed for OFDM systems (e.g., IEEE 802.11a system) based on Fountain codes and resolution-adaptive ADCs. Each Fountain-encoded packet is transmitted over a subcarrier. By discarding Fountain-encoded packets that have been transmitted over “bad” subcarriers, the dynamic range of ADCs can be reduced. Correspondingly, the power consumption of ADCs can be lowered as well.

The ADCs in a receiver can consume up to 50% of the total baseband energy, so it is advantageous to lower its power consumption. The resolution-adaptive ADC can save on average around 42% energy consumption comparing to the conventional ADC. Fountain codes together with LDPC plus CRC codes can allow the power consumption in ADC to be decreased by an additional 30%. So, the new opportunistic error-correction layer can reduce the power consumption in ADC by more than 70% compared with the conventional IEEE 802.11a system. In addition, it requires 7.5 dB less SNR than the 802.11a system.

Besides, we have shown that the new error-correction layer is a robust scheme against the channel estimation errors. So, ADCs can also be adapted to the minimum resolution in a realistic system where the channel is estimated. Moreover, by using message-passing algorithm and Gaussian elimination algorithm, the new error-correction scheme can be applied to a small packet size (e.g.,  $K = 500$ ) with low overhead (e.g., 3%) which can make this new scheme efficient.

Here, we assume that there is no adjacent interference which does not happen in the real wireless channels. Further research focuses on the optimization of this new error-correction for the wireless channel with adjacent interference.

## Acknowledgments

The authors thank the anonymous reviewers for the useful comments. Also, the authors thank the Dutch Ministry of Economic Affairs under the IOP Generic Communication—SenterNovem Program for the financial support.

## References

- [1] A. Bahai, B. Saltzberg, and M. Ergen, *Multi-Carrier Digital Communications: Theory and Applications of OFDM*, Springer, New York, NY, USA, 2004.
- [2] H. Liu and G. Li, *OFDM-Based Broadband Wireless Networks: Design and Optimization*, John Wiley & Sons, New York, NY, USA, 2005.
- [3] M. Engels, *Wireless OFDM Systems: How to Make Them Work?* Kluwer Academic Publishers, Dordrecht, The Netherlands, 2002.
- [4] D. Tse and P. Viswanath, *Fundamentals of Wireless Communication*, Cambridge University Press, New York, NY, USA, 2005.
- [5] J. Thomson, B. Baas, E. M. Cooper, et al., “An integrated 802.11a baseband and MAC processor,” in *Proceedings of the IEEE International on Solid-State Circuits Conference (ISSCC '02)*, vol. 1, pp. 126–451, San Francisco, Calif, USA, February 2002.
- [6] IEEE 802.11a-1999, “Supplement to Information Technology—Telecommunications and Information Exchange Between Systems—Local and Metropolitan Area Networks—Specific Requirements—Part 11: Wireless LAN Medium Access Control and Physical Layer Specifications: High Speed Physical Layer in the 5 GHz Band,” November 1999.
- [7] D. J. C. MacKay, “Fountain codes,” *IEEE Proceedings: Communications*, vol. 152, no. 6, pp. 1062–1068, 2005.
- [8] M. Luby, “LT codes,” in *Proceedings of the 43rd Annual IEEE Symposium on Foundations of Computer Science*, pp. 271–280, Vancouver, Canada, November 2002.
- [9] A. Shokrollahi, “Raptor codes,” *IEEE Transactions on Information Theory*, vol. 52, no. 6, pp. 2551–2567, 2006.
- [10] H. Zhu, C. Zhang, and J. Lu, “Designing of fountain codes with short code-length,” in *Proceedings of the 3rd International Workshop on Signal Design and Its Applications in Communications (IWSDA '07)*, pp. 65–68, Chengdu, China, September 2007.
- [11] X. Shao, R. Schiphorst, and C. H. Slump, “Opportunistic error correction for WLAN applications,” in *Proceedings of the International Conference on Wireless Communications, Networking and Mobile Computing (WiCOM '08)*, pp. 1–5, Dalian, China, October 2008.
- [12] A. Bogdanov, M. C. Mertens, C. Paar, J. Pelzl, and A. Rupp, “A parallel hardware architecture for fast Gaussian elimination over GF(2),” in *Proceedings of the 14th Annual IEEE Symposium on Field-Programmable Custom Computing Machines (FCCM '06)*, pp. 237–248, Napa, Calif, USA, April 2006.
- [13] Y. Kou, S. Lin, and M. P. C. Fossorier, “Low-density parity-check codes based on finite geometries: a rediscovery and new results,” *IEEE Transactions on Information Theory*, vol. 47, no. 7, pp. 2711–2736, 2001.
- [14] C. Berrou, A. Glavieux, and P. Thitimajshima, “Near Shannon limit error-correcting coding and decoding: turbo-codes. 1,” in *Proceedings of the IEEE International Conference on Communications (ICC '93)*, vol. 2, pp. 1064–1070, Geneva, Switzerland, May 1993.
- [15] E. Jacobsen, “LDPC FEC for 802.11n application,” IEEE, 2003.
- [16] J. G. Proakis, *Digital Communications*, McGraw Hill, New York, NY, USA, 2001.
- [17] S. Nahata, K. Choi, and J. Yoo, “A high-speed power and resolution adaptive flash analog-to-digital converter,” in *Proceedings of the IEEE International SOC Conference*, pp. 33–36, Santa Clara, Calif, USA, September 2004.
- [18] X. Shao and C. H. Slump, “Quantization effects in OFDM systems,” in *Proceedings of the 29th Symposium on Information Theory in the Benelux*, pp. 93–103, Leuven, Belgium, May 2008.
- [19] S. M. Ross, *Introduction to Probability Models*, Academic Press, Orlando, Fla, USA, 2003.
- [20] A. Doufexi, S. Armour, M. Butler, et al., “A comparison of the Hiperlan/2 and IEEE 802.11a wireless LAN standards,” *IEEE Communications Magazine*, vol. 40, no. 5, pp. 172–180, 2002.

## Special Issue on Advanced Signal Processing for Cognitive Radio Networks

### Call for Papers

Cognitive radio is widely expected to usher in the next wave in wireless communications. In December 2003, the Federal Communications Commission (FCC) of the US government issued authorized cognitive radio techniques for spectrum sharing/reusing and approved the use of fixed and mobile services in TV bands. In October 2008, the FCC further approved the use of mobile white space devices in TV bands, and many governments worldwide have also moved to support this new spectrum usage model. This has been accompanied recently by a significant upsurge in academic research and application initiatives, such as the IEEE 802.22 standard on wireless regional area networks (WRANs) and the Wireless Innovation Alliance including Google and Microsoft as members, which advocates unlocking the potential in the “white space” of television bands.

However, cognitive radio networking is still in the early stages of research and development. To achieve full “cognition” and reliable communication over a wireless network, there are still tremendous technical, economical, and regulatory challenges. Signal processing plays a major role in cognitive radio networks. The aim of this special issue is to present a collection of high-quality research papers in advanced signal processing for cognitive radio including theoretical studies, algorithms, protocol design, as well as architectures, platforms, and prototypes which use advanced signal processing techniques. Topics of interest include, but are not limited to:

- Advanced spectrum sensing techniques and protocol support
- Cooperative spectrum sensing and communication
- Resource allocation for spectrum sharing
- Exploiting multiantennas for spectrum sharing
- Channel and environment learning techniques for cognitive radio
- Advanced coding and modulation for cognitive radio
- Information theory for cognitive radio
- Multiuser spectrum access techniques
- Security issues in cognitive radio networks
- Multimedia transmission over cognitive radio networks

- Optimization for bandwidth utilization
- Cognitive radio prototypes and test beds

Before submission authors should carefully read over the journal’s Author Guidelines, which are located at <http://www.hindawi.com/journals/asp/guidelines.html>. Prospective authors should submit an electronic copy of their complete manuscript through the journal Manuscript Tracking System at <http://mts.hindawi.com/>, according to the following timetable:

Manuscript Due	May 1, 2009
First Round of Reviews	August 1, 2009
Publication Date	November 1, 2009

### Lead Guest Editor

**Ying-Chang Liang**, Institute for Infocomm Research, A\*STAR, 1 Fusionopolis Way, No.21-01 Connexis (South Tower), Singapore 138632; [yliang@i2r.a-star.edu.sg](mailto:yliang@i2r.a-star.edu.sg)

### Guest Editors

**Xiaodong Wang**, Department of Electrical Engineering, Columbia University, 717 Schapiro CEPSR, 500 West 120th Street, New York, NY 10027, USA; [wangx@ee.columbia.edu](mailto:wangx@ee.columbia.edu)

**Yonghong Zeng**, Institute for Infocomm Research, A\*STAR, 1 Fusionopolis Way, No. 21-01 Connexis (South Tower), Singapore 138632; [yhzeng@i2r.a-star.edu.sg](mailto:yhzeng@i2r.a-star.edu.sg)

**Jinho Choi**, Wireless Group, Swansea University, Singleton Park, Swansea, SA2 8PP Wales, UK; [J.Choi@swansea.ac.uk](mailto:J.Choi@swansea.ac.uk)

**Rui Zhang**, Institute for Infocomm Research, A\*STAR, 1 Fusionopolis Way, No. 21-01 Connexis (South Tower), Singapore 138632; [rzhang@i2r.a-star.edu.sg](mailto:rzhang@i2r.a-star.edu.sg)

**Marco Luise**, Dipartimento di Ingegneria dell’Informazione, Università degli studi di Pisa, 56100 Pisa, Italy; [marco.luise@iet.unipi.it](mailto:marco.luise@iet.unipi.it)

## Special Issue on CMOS Application to Wireless Communications

### Call for Papers

Recent advances in semiconductor process technologies have motivated the development of fully integrated CMOS circuits for wireless communications. Consequently, tremendous research efforts have been directed to the design and implementation of CMOS radio-frequency integrated circuits (RFICs). The objective of this special issue is to highlight the up-to-date progress in the field of CMOS RF devices and circuits.

The International Journal of Microwave Science and Technology invites authors to submit papers for the special issue on CMOS RF. Original papers previously unpublished and not currently under review by another journal are solicited for this special issue. Topics of interest include, but are not limited to:

- CMOS and BiCMOS RF device technologies
- Small-signal circuits
- Large-signal circuits
- Mixed-signal circuits
- Millimeter-wave integrated circuits
- Signal generation circuits
- Frequency-conversion circuits
- Wide-band integrated circuits
- Cellular system IC's and architecture
- Emerging RF applications
- Modeling and CAD

Before submission, authors should carefully read over the journal's Author Guidelines, which are located at <http://www.hindawi.com/journals/ijmst/guidelines.html>. Prospective authors should submit an electronic copy of their complete manuscript through the journal Manuscript Tracking System at <http://mts.hindawi.com/>, according to the following timetable:

Manuscript Due	September 1, 2009
First Round of Reviews	December 1, 2009
Publication Date	March 1, 2010

### Lead Guest Editor

**Liang-Hung Lu**, Department of Electrical Engineering, National Taiwan University, Roosevelt Road, Taipei 106, Taiwan; [lhlu@cc.ee.ntu.edu.tw](mailto:lhlu@cc.ee.ntu.edu.tw)

### Guest Editor

**Huei Wang**, Department of Electrical Engineering, National Taiwan University, Roosevelt Road, Taipei 106, Taiwan; [hueiwang@ntu.edu.tw](mailto:hueiwang@ntu.edu.tw)